

Supplementary information

Lithium-Doping Inverts the Nanoscale Electric Field at the Grain Boundaries in $\text{Cu}_2\text{ZnSn}(\text{S},\text{Se})_4$ and Increases Photovoltaic Efficiency

H. Xin^{a,d}, S. M. Vorpahl^{b,d}, A. D. Collord^{a,d}, I. L. Braly^{a,d}, A. R. Uhl^{a,d}, B. W. Krueger^c, D. S. Ginger^{b,d}, and H. W. Hillhouse^{a,d*}

Recrystallization of thiourea.

Thiourea was dissolved in 90 °C DI water under stirring to near saturation. The hot solution was filtered under vacuum from a funnel with filtering paper. The solute was naturally cooled down to room temperature and white crystals precipitated. The crystals were filtered using a filtering paper, washed with DI and dried at room temperature in ambient air.

Li doping concentration study.

Table S1. CZTSSe Solar cell performance as a function of LiF concentration in the precursor ink. The device parameters presented for each sample are average values with standard deviations from 15 solar cells with an active area of 0.10 cm² without antireflective coating.

Li/(Cu+Zn+Sn) (%) ^a	J _{sc} (mA/cm ²)	V _{oc} (V)	FF (%)	PCE (%)	n	R _s (Ω cm ²)	R _{sh} (Ω)
0	32.23±0.6	0.426±0.011	57.8±2.6	7.93±0.47	2.25±0.16	0.53±0.11	2781±117
0.001	30.05±1.81	0.434±0.013	58.1±2.7	7.58±0.93	2.49±0.26	0.55±0.06	5218±191
0.01	32.51±0.65	0.448±0.006	63.5±2.4	9.25±0.45	1.99±0.28	0.43±0.05	4497±138
0.1	32.30±0.89	0.445±0.004	60.9±3.3	8.77±0.59	2.07±0.08	0.56±0.16	4019±123
1.0	34.15±0.80	0.448±0.003	65.6±0.9	10.04±0.35	1.84±0.05	0.38±0.02	4096±54

a. Atomic ratio of Li to all the metal ions.

Solar cell characterization. Current-voltage (J-V) measurements were performed using a Keithley 2400 source-measure unit in the dark and under 100 mW/cm² simulated AM1.5G illumination from a xenon arc lamp with an AM1.5G filter. The incident power was calibrated with a Newport Si reference cell. Each device has an active area of around 0.10 cm². However, the exact area for each device was determined using an optical microscope with a distance calibration standard and used for all current density calculations. External quantum efficiency

was measured using a chopped monochromatic beam and lock-in amplifier. Calibrated Si and Ge photodiodes were used as references for EQE measurements.

Scanning electron microscopy. Surface and cross-section scanning electron microscopy (SEM) images and energy dispersive X-ray spectroscopy (EDS) data of the CZTSSe film were collected with an FEI Sirion system at the NanoTech User Facility (NTUF) at the Center for Nanotechnology University of Washington (UW). Top view images were measured on bare CZTSSe films that were prepared in parallel to the solar cell devices. Cross-section images were conducted on cleaved devices.

X-ray diffraction. The X-ray diffraction of the CZTSSe films was measured on a Bruker D8 Focus diffractometer using Cu K α radiation ($\lambda = 0.15406$ nm) at a scanning speed of $0.05^\circ/\text{s}$. Films for XRD measurements were prepared in parallel to that for solar cell devices.

X-ray diffraction patterns of the CZTSSe films processed with and with LiF are shown in Figure S1. The texture of the CZTSSe films are determined by the Lotgering factors $f(hkl)$. A Lotgering factor $f(hkl)$ equal to unity indicates that the film has an (hkl) orientation. A value of zero corresponds to a polycrystalline film with a random texture. According to Hanna,¹ CIGS films with $f(112) \leq |0.2|$ and $f(220/204) \leq |0.2|$ have random texture. A random texture implies a random distribution of crystallite orientations. The Lotgering factors of $f(112)$ and $f(220/204)$ are calculated to be -0.03 and 0.04 for film without Li doping and -0.1 and 0.03 for doped film, both have random texture.

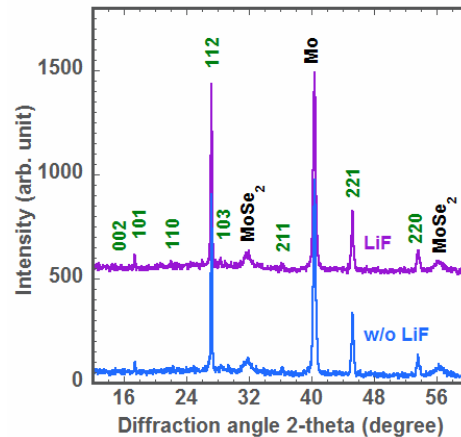


Fig.S1. X-ray diffraction of CZTSSe films processed with and without LiF. The intensity is normalized to the Mo diffraction peak.

Inductively coupled plasma-mass spectroscopy. Elemental concentrations of Li were determined by inductively coupled plasma-mass spectroscopy (ICP-MS) using a PerkinElmer ELAN DRC-e. Li and Cu standards were prepared by diluting certified stock solutions (1000 mg/l, Fluka Analytical) with matrix matching, Cu and Li were calibrated from 2 $\mu\text{g/l}$ to 20 mg/l and from 0.02 $\mu\text{g/l}$ to 2 mg/l, respectively. Solid samples of precursor CZTS films and selenized CZTSSe films were scratched off the Mo-coated SLG substrate with borosilicate pipettes and digested in HCl/HNO₃ solutions (trace metal grade: 99.999%). The measurements were carried out in dynamic reaction cell (DRC) mode with NH₃ gas and optimized rinse durations between samples to allow for unambiguous quantification of Li.

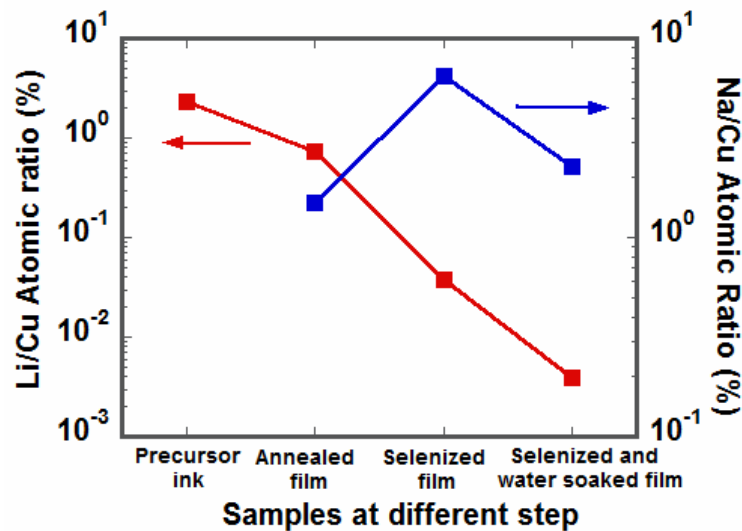


Figure S2. Li/Cu and Li/Na ratios derived from the ICP-MS of Li-doped films at different stages. The value in the precursor ink is the feed in ratio.

The Li/Cu and Na/Cu ratios measured from the scratched Li-doped films at different stages are shown in Fig. S2. The Li/Cu and Na/Cu ratios for the as-annealed, as-selenized, and H₂O soaked selenized films are 7.3×10^{-3} , 3.8×10^{-4} , and 3.9×10^{-5} , and 1.49×10^{-2} , 6.49×10^{-2} , and 2.29×10^{-2} , respectively. The more than half reduced Na after H₂O soaking confirms a great amount of Na on film surface, which is consistent with the XPS data (Fig. S2) as will be discussed below.

To test the experimental error, the ICP-MS of Li from an annealed and non-Li film was measured. The Li/Cu ratio derived from the ICP-MS data is 8.88×10^{-6} , which is close to the instrument test limit and three orders magnitude lower than that from Li-doped film (7.31×10^{-3}), indicating the validity of our measurements. The results at the same time confirm that the Li is indeed from dopant (not substrate). In addition, the ICP-MS of a non-Li film after thermal annealing was also tested. The Na/Cu ratio derived from the ICP is 7.95×10^{-3} , which is comparable to that from Li-doped film (1.49×10^{-2}).

X-ray photoelectron spectroscopy.

X-ray photoelectron spectroscopy (XPS) was conducted on a PHI Versaprobe 5000 spectrometer with monochromatic Al K α (1,486.6 eV) radiation. Data were collected at 45° takeoff angle using a 23.5 eV pass energy and an energy step of 0.025 eV. Charge neutralization was accomplished by flooding the sample surface with low energy electrons during data acquisition, and any resulting variations were subsequently removed by shifting all spectra to align the Cu 2p_{3/2} peak to 931.9 eV (adventitious carbon was not used as a charge reference due to the overlapping Se LMM Auger peak). After shifting, binding energies of Zn 2p_{3/2}, Sn 4d_{5/2}, Se 3p_{3/2}, and Se 3d_{5/2} peaks are 1021.6 eV, 486.0 eV, 160.2 eV, and 53.8 eV, respectively.

The X-ray photoelectron spectra of the CZTSSe films with and without Li doping before and after water soaking are shown in Figure S3. A significant amount of sodium (Na 1s) is present on the surface of the film with lithium doping, but it is washed away by DI water soaking. No sodium signal is detected on the film processed without LiF. We note that in another set of films, a weak signal from Na was detected on the surface of non-Li film and a strong Na signal was detected for the lithium doped sample, suggesting that lithium affects the mechanism of sodium migration to the surface. This is an interesting finding that is the focus of ongoing experiments. From Figure S3 (b) and (c), the Se 3p and Se 3d XPS peaks, we see that H₂O soaking does not appear to have any effect on non-Li CZTSe films. However, films doped with lithium show a significant change in the shape of the Se 3d spectrum, but not in Se 3p. This is attributed to intensity from the Li 1s and not an additional Se component. Different samples had differing amounts of adventitious carbon on the surface which attenuated the signal from the CZTSe film underneath, so the spectra have been scaled to compensate.

To estimate the amount of lithium on the surface of the Li-treated film, a subtraction procedure was employed to remove the Se 3d contribution and reveal the Li 1s contribution. First the spectra were shifted according to Cu 2p_{3/2}, and the Shirley background was subtracted from each spectrum. Next the H₂O-soaked sample was scaled to compensate for the observed C 1s contamination layer, where the scaling factor was determined by requiring that the difference remains positive. Finally the subtraction was performed, and the resulting difference was fit to two Voigt profiles. The result of this procedure is shown in Fig. S3(d). Two Li components are present, one at 54.4 eV (Li 2) and one at 55.3 eV (Li 1). Of the published values for Li compounds, the two peaks line-up most closely with LiOH² for the lower binding energy peak and Li₂O² (or possibly Li₂Se³) for the higher binding energy peak. However, other yet to be determined species may be present and responsible for the Li 1s signal.

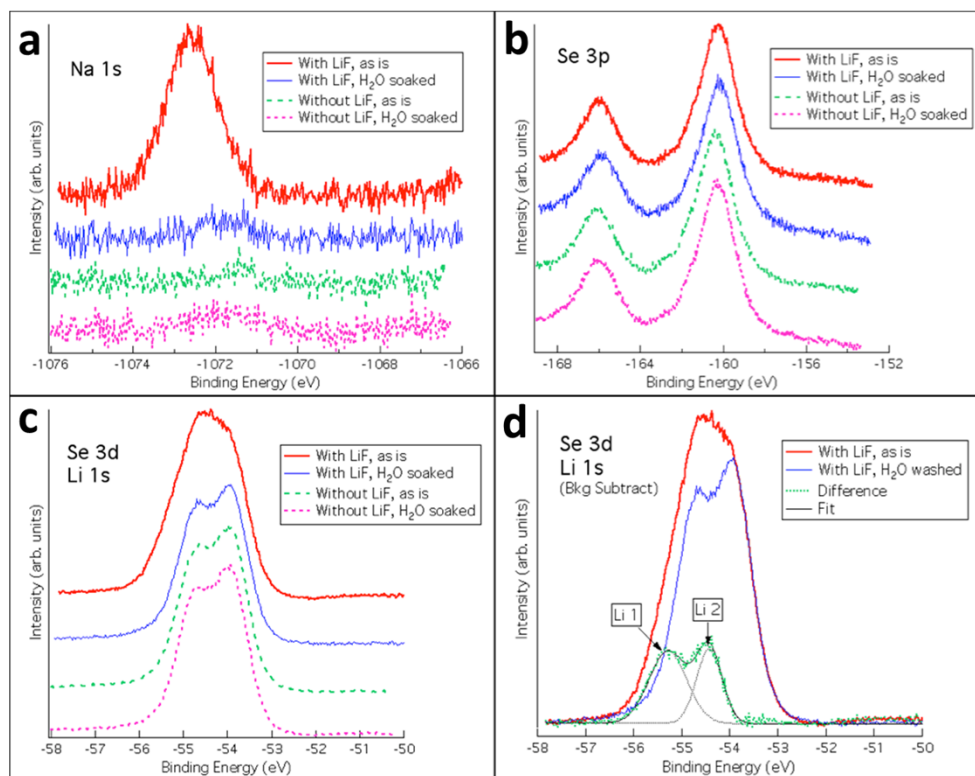


Figure S3. X-ray photoelectron spectra of CZTSSe films with and without LiF before and after H₂O soaking. (a) Na 1s peaks; (b) Se 3p peaks; (c) Se 3d/Li 1s peaks and (d) curve fittings of Se 3d/Li 1s peak of Li- doped film.

Scanning Probe Microscopy.

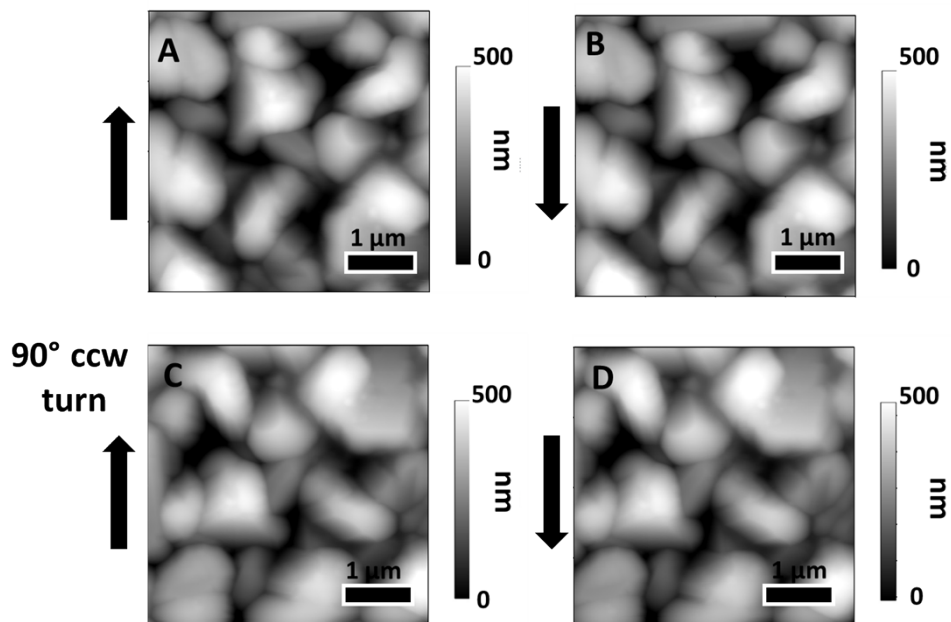


Figure S4. Consecutive AFM topography scans taken in contact mode showing no damage to crystals. Scan A and B taken at 0°. Scan C and D taken at 90° counterclockwise turn.

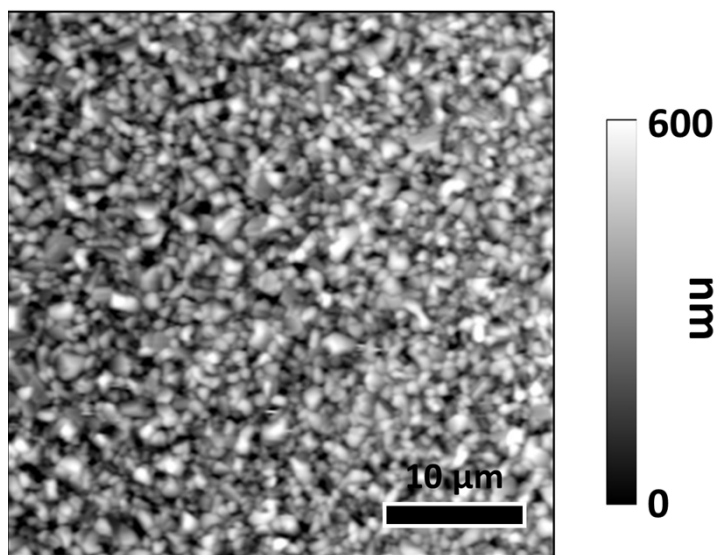


Figure S5. 40 μm x 40 μm AFM topography scan taken in contact mode showing no damage to crystals over very large scan area.

Drive-Level Capacitance Profiling.

Room temperature drive-level capacitance profiling (DLCP) experiments⁴ were carried out using a Solartron 1260 impedance analyzer. Impedance measurements were made by sweeping frequency, AC voltage (keeping the peak voltage at the same absolute level), and DC voltage (the peak of the AC variation) in this respective hierarchy. Frequencies ranging from 0.1 to 100 kHz, peak-to-peak AC voltages ranging from 7.1 to 424.3 mV, and DC voltages ranging from -0.5 to 0.5 V were used. Devices were measured in an aluminum faraday cage with BNC feed-throughs. The total device area is assumed to be the planar interface area, and the relative dielectric value is taken to be 8.5 (based on the theoretical value of the pure selenide).^{5, 6} Methods used to calculate DLCP-determined charge-response density have been described previously.⁷

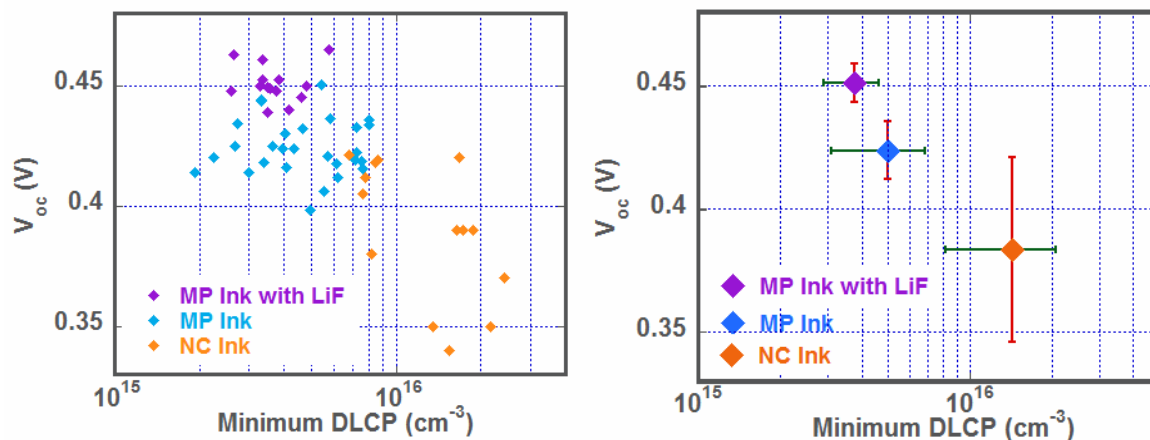


Figure S6. Correlation of device open-circuit voltages versus DLCP concentrations, $N_{\text{DLCP,min}}$. MP ink: molecular precursor ink. NC ink: nanocrystal ink.

References

1. G. Hanna, T. Glatzel, S. Sadewasser, N. Ott, H. P. Strunk, U. Rau and J. H. Werner, *Appl. Phys. A*, 2006, **82**, 1-7.
2. J. P. Contour, A. Salesse, M. Froment, M. Garreau, J. Thevenin and D. Warin, *Journal De Microscopie Et De Spectroscopie Electroniques*, 1979, **4**, 483-491.
3. M. Kamaratos, D. Vlachos, C. A. Papageorgopoulos, A. Schellenberger, W. Jaegermann and C. Pettenkofer, *J. Phys.: Condens. Matter*, 2002, **14**, 8979-8986.
4. J. T. Heath, J. D. Cohen and W. N. Shafarman, *J. Appl. Phys.*, 2004, **95**, 1000-1010.
5. C. Persson, *J. Appl. Phys.*, 2010, **107**.
6. O. Gunawan, T. Gokmen, C. W. Warren, J. D. Cohen, T. K. Todorov, D. A. R. Barkhouse, S. Bag, J. Tang, B. Shin and D. B. Mitzi, *Appl. Phys. Lett.*, 2012, **100**, 253905-253904.
7. H. Xin, J. K. Katahara, I. L. Braly and H. W. Hillhouse, *Adv. Energy Mater.* 2014, **4**, 201301823.